



(0 0 0) and (0 1 0) energy levels of the HD¹⁸O and D₂¹⁸O molecules from analysis of their ν_2 bands

An-Wen Liu^a, Ke-Feng Song^a, Hong-Yu Ni^a, Shui-Ming Hu^a, Olga V. Naumenko^{b,*}, Irina A. Vasilenko^b, Semen N. Mikhailenko^b

^aHefei National Laboratory for Physical Sciences at Microscale, University of Science and Technology of China, Hefei 230026, China

^bLaboratory of Theoretical Spectroscopy, V.E. Zuev Institute of Atmospheric Optics, SB RAS, 1, Akademichan Zuev Square, 634021 Tomsk, Russia

ARTICLE INFO

Article history:

Received 21 June 2010

Available online 3 December 2010

Keywords:

Fourier transform spectroscopy

Water molecule

Absorption spectrum

HD¹⁸O

D₂¹⁸O

Rotation-vibration assignments

ABSTRACT

High-resolution Fourier-transform spectra of water samples enriched by deuterium and oxygen-18 at room temperature are analyzed in the range 969–2148 cm⁻¹. Line positions of about 2470 transitions up to $J_{max} = 22$ and $K_a_{max} = 12$ of the ν_2 bands of the HD¹⁸O and D₂¹⁸O molecules are reported. This has allowed the determination of extended sets of rotational energies of the (0 0 0) and (0 1 0) vibrational states for both molecules. The generation function model of an effective rotational Hamiltonian was used in the data reduction to account for the strong centrifugal distortion of the rotational levels. Values of effective Hamiltonian parameters have been determined. The RMS standard deviations of the least-squares fits of the energy levels were 2.4×10^{-4} cm⁻¹ for 293 energy levels of the ground state and 3.2×10^{-4} cm⁻¹ for 281 energy levels of the (010) state of D₂¹⁸O, and 2.6×10^{-4} cm⁻¹ for 227 energy levels of the ground state and 4.2×10^{-4} cm⁻¹ for 246 energy levels of the (0 1 0) state of HD¹⁸O. Comparisons of obtained data with the theoretical predictions as well as with other observations are presented.

© 2010 Elsevier Inc. All rights reserved.

1. Introduction

Study of the high resolution rovibrational spectra of the water vapor isotopic species is of continuous interest during last two decades. Recently, an exhaustive analysis of the H₂¹⁸O, H₂¹⁷O, HD¹⁶O, HD¹⁸O, HD¹⁷O, and D₂¹⁸O published rotation-vibrational transitions have been performed, and consistent sets of the experimental energy levels have been derived based on the Rydberg–Ritz principle [1–4]. Rare isotopic species of the water molecule, like HD¹⁸O, and, especially, D₂¹⁸O are much less investigated compared to other more abundant isotopologues. Complete list of the available studies can be found in [1,3] for HD¹⁸O and in [4,5] for D₂¹⁸O. Even for the lowest vibrational states (0 0 0) and (0 1 0), the experimental sets of rotational energy levels were limited (until recent study for D₂¹⁸O [5]), by $J \leq 16$ and $K_a \leq 10$. Accurate experimental rotational energy levels of the (0 0 0) and (0 1 0) states represent the initial and essential information for determination of all the upper

experimental levels in room temperature spectra. The present study is aimed at improving and enlarging the set of experimental energy levels of the (0 0 0) and (0 1 0) states of the D₂¹⁸O and HD¹⁸O molecules using newly recorded high resolution Fourier transform spectra in the 969–2148 cm⁻¹ spectral range combined with all previously published rotation-vibrational transitions of these two water isotopologues. The (0 0 0) and (0 1 0) rotational energy levels have been derived from solution of the system of the Rydberg–Ritz linear equations which includes all validated rotation-vibrational transitions.

2. Experimental details

The spectra were recorded with a Bruker IFS 120 HR Fourier transform spectrometer in Hefei. Experimental details of the measurements have been presented in our previous papers [5,6]. Here we just give a brief summary of the experimental conditions.

The enriched D₂¹⁸O water sample used in the measurements was purchased from ICON Services. The stated isotopic concentration of ¹⁸O is 98%. The spectrum region was extended down to 970 cm⁻¹. A global source, a liquid nitrogen cooled MCT detector, and a KBr beam-splitter were used. The unapodized spectral resolution was 0.005 cm⁻¹. A 1.5-m base path length adjustable

* Corresponding author. Address: Laboratory of Theoretical Spectroscopy, V.E. Zuev Institute of Atmospheric Optics, Russian Academy of Sciences, 1, Akademichan Zuev Square, 634021 Tomsk, Russia. Fax: +7 382 2 49 20 86.

E-mail address: olga@asd.iao.ru (O.V. Naumenko).

multi-pass gas cell operated at room temperature was used. Total path length for the spectra recording was 15 m. The sample pressure was measured with two capacitance manometers (MKS Baratron 627B) of 1 torr and 20 torr full-scale ranges with an overall accuracy of 0.15%. The sample pressures were 38 and 1520 Pa. Different optical filters were applied to improve the signal-to-noise ratio and to allow the high resolution measurements. The line posi-

tions were calibrated using the absorption lines of H_2^{16}O and HD^{16}O . Their values were taken from the *HITRAN* 2008 database [7]. The accuracy of the line positions of unblended and not-very-weak lines was estimated to be better than $2 \times 10^{-4} \text{ cm}^{-1}$.

Two examples of the recorded spectra near 1176 cm^{-1} (upper panel) and 1583 cm^{-1} (lower panel) with the rotation-vibration assignments are shown in Fig. 1.

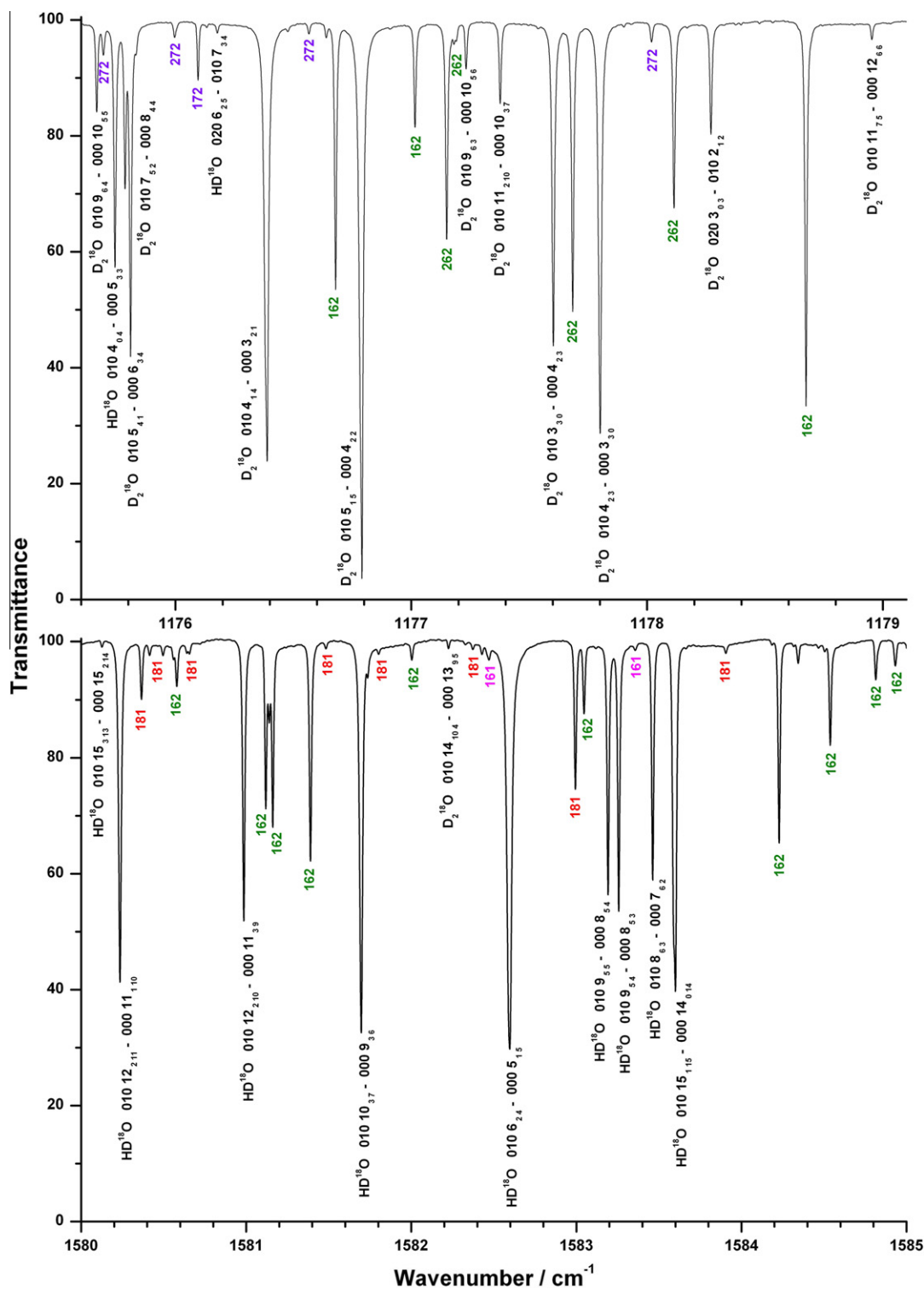


Fig. 1. Part of the spectrum near 1176 cm^{-1} (upper panel) and near 1583 cm^{-1} (lower panel). Rotation-vibration assignments are given for the HD^{18}O and D_2^{18}O lines. Lines of other water species are marked by the code of molecule: 161 – H_2^{16}O , 162 – HD^{16}O , 262 – D_2^{16}O , 181 – H_2^{18}O , 172 – HD^{17}O , and 272 – D_2^{17}O .

3. Results and discussion

3.1. Spectrum assignment

The assignment of experimental spectra recorded in 969–2148 cm^{-1} region has been performed using the accurate variational computations [8] based on Partridge and Schwenke potential energy surface [9] and Schwenke and Partridge dipole moment function [10]. Hereinafter calculated spectra from [8] will

be referred to as PS data (PS energy levels, PS line positions, PS line intensities). It turned out that PS and experimental energy levels for the (0 1 0) state agree very well both for D_2^{18}O and HD^{18}O , what is illustrated in Fig. 2. Maximum *obs-cal* deviations were found to be of 0.16 and -0.08 cm^{-1} , and RMS deviations equal to 0.055 and 0.040 cm^{-1} for HD^{18}O and D_2^{18}O , respectively. Deviations of the PS energy levels of the ground states from the observed data are also included in Fig. 2 for both considered molecules. Typical regular structure of the *obs-cal* deviations can be easily found in

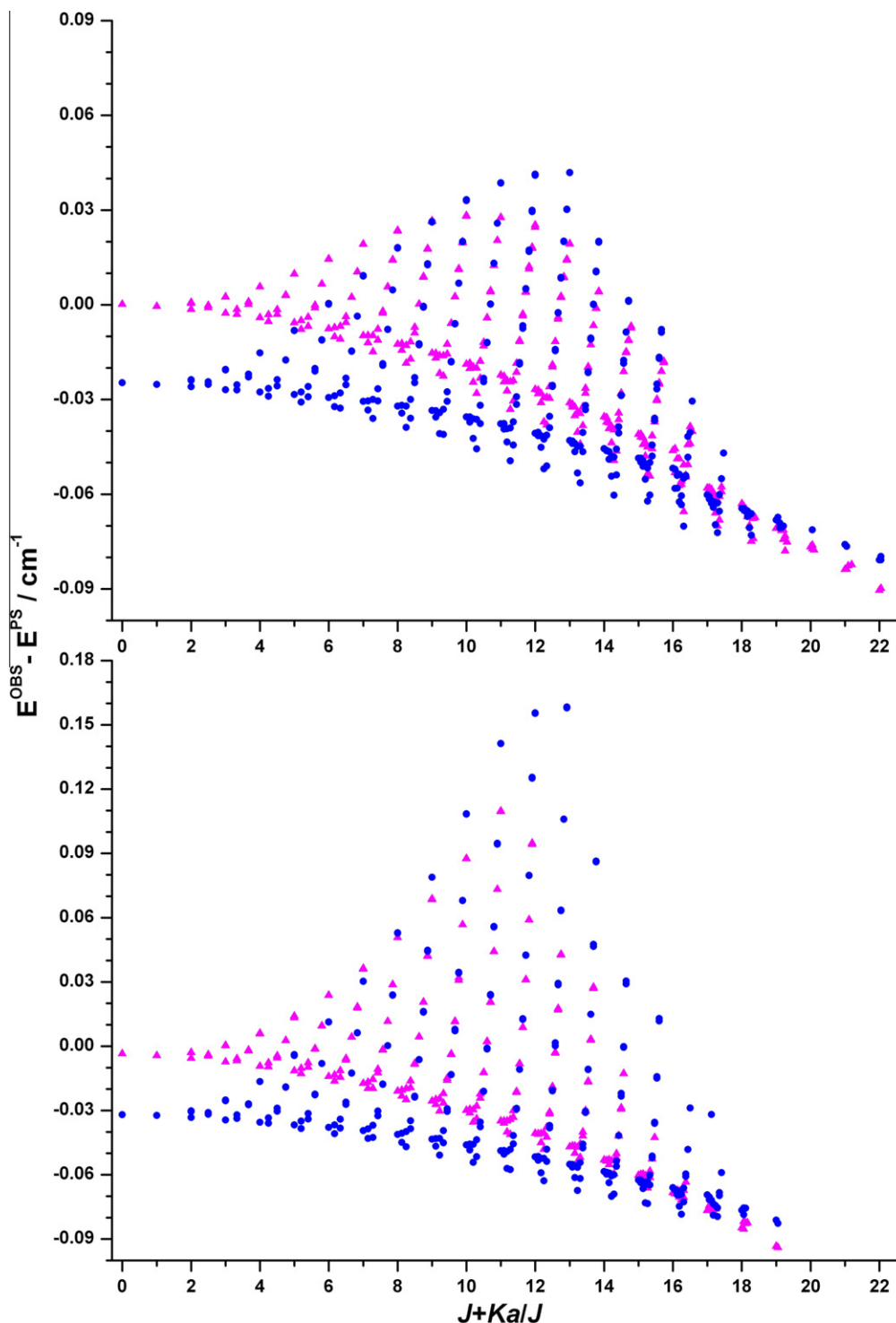


Fig. 2. Discrepancies between the experimental (E^{OBS}) and calculated (E^{PS}) energies for D_2^{18}O (upper panel) and HD^{18}O (lower panel). Discrepancies for the ground states are given by triangles. Discrepancies for the (0 1 0) states are given by circles.

Table 1

Summary of experimental sources for the D₂¹⁸O data used to retrieve energy levels from transitions.

Spectral region (cm ⁻¹)	Number of transitions		Reference
	Total	Selected ^a	
0.2968–12.5557	21	21	[11]
19.8843–37.5600	8	2	[12]
34.5178–216.3729	144	143	[13]
953.309–1453.719	507	506	[14]
969.135–1605.474	1154	1145	This study
971.308–1684.135	45	13	[15]
974.389–1443.467	138	132	[16]
2088.501–3217.693	2905	2889	[5]
2594.842–2917.267	303	282	[17]
6127.288–8245.646	277	122	[4]
Total	5502	5255	

^a Number of transitions included in the energy levels determination.

Table 2

Experimental energy levels for the ground and (0 1 0) states of D₂¹⁸O and HD¹⁸O.

J _{Ka} Kc	D ₂ ¹⁸ O				HD ¹⁸ O			
	(0 0 0)		(0 1 0)		(0 0 0)		(0 1 0)	
	E ^{OBS}	δE	E ^{OBS}	δE	E ^{OBS}	δE	E ^{OBS}	δE
0 0 0			1170.15729	36			1396.26639	8
1 0 1	12.08203	16	1182.24816	22	15.41842	8	1411.73581	6
1 1 1	19.87760	16	1191.15935	22	29.45975	6	1427.69235	6
1 1 0	22.33847	16	1193.73743	24	32.14882	8	1430.59234	6
2 0 2	35.74246	20	1205.93930	20	45.89839	4	1442.30643	4
2 1 2	41.58219	16	1212.76578	20	57.59726	4	1455.72021	4
2 1 1	48.95900	16	1220.49347	20	65.65885	4	1464.41355	4
2 2 1	72.26100	18	1247.09404	20	107.63032	2	1512.01078	4
2 2 0	72.75734	12	1247.57672	18	107.97917	4	1512.36892	4
3 0 3	70.10194	16	1240.35958	20	90.76520	4	1487.28117	4
3 1 3	73.84413	12	1244.88626	16	99.58688	4	1497.53949	2
3 1 2	88.51550	16	1260.26391	18	115.66495	2	1514.87761	4
3 2 2	108.51317	12	1283.37887	16	153.82193	2	1558.35340	2
3 2 1	110.86621	14	1285.68184	22	155.52603	2	1560.10612	2
3 3 1	153.47950	10	1333.96838	14	230.20191	4	1644.26275	4
3 3 0	153.54393	16	1334.02646	18	230.23080	4	1644.29059	4
4 0 4	114.30815	12	1284.62064	14	149.18777	2	1545.78813	2
4 1 4	116.39397	14	1287.25177	18	155.20823	2	1552.92145	2
4 1 3	140.47778	12	1312.53966	16	181.81788	2	1581.62669	2
4 2 3	156.42452	14	1331.34381	16	215.10969	2	1619.83429	2
4 2 2	162.81888	10	1337.66371	14	219.97924	2	1624.85865	2
4 3 2	202.66301	14	1383.19218	16	292.30915	2	1706.58704	4
4 3 1	203.09986	12	1383.58729	14	292.50603	2	1706.77931	2
4 4 1	263.87422	12	1451.97676	16	397.42826	4	1824.30269	4
4 4 0	263.88128	10	1451.98269	16	397.42942	4	1824.30399	4
5 0 5	167.93242	14	1338.22184	16	220.46393	2	1617.06470	2
5 1 5	168.98230	10	1339.60618	14	224.22298	2	1621.61781	2
5 1 4	204.04141	14	1376.54881	14	263.59302	2	1664.12591	2
5 2 4	215.65559	12	1390.65482	14	291.24216	2	1696.19508	2
5 2 3	228.63441	14	1403.62341	16	301.74477	2	1707.08203	2
5 3 3	264.17810	10	1444.77111	12	370.04456	2	1784.60112	2
5 3 2	265.82606	12	1446.27157	18	370.81443	2	1785.35426	2
5 4 2	325.45906	12	1513.61441	14	474.88954	2	1902.02445	4
5 4 1	325.52011	14	1513.66561	16	474.90656	2	1902.04034	2
5 5 1	403.03348	12	1600.44505	18	608.47285	4	2050.72941	4
5 5 0	403.03405	14	1600.44537	20	608.47285	4	2050.72943	6
6 0 6	230.92083	10	1401.06224	14	304.21938	2	1700.67863	2
6 1 6	231.41580	14	1401.74468	18	306.40761	2	1703.39257	2
6 1 5	278.19601	10	1451.29619	16	360.26396	2	1761.63675	2
6 2 5	285.82477	14	1460.93398	18	381.91861	2	1787.12673	2
6 2 4	307.81955	10	1483.13493	14	400.81549	2	1806.81576	2
6 3 4	337.85625	12	1518.55523	16	463.36149	2	1878.26414	2
6 3 3	342.33760	10	1522.68399	12	465.58309	2	1880.44222	2
6 4 3	399.54702	14	1587.76071	16	568.00177	2	1995.45117	2
6 4 2	399.83918	12	1588.00671	14	568.08582	2	1995.52942	2
6 5 2	476.94793	14	1674.44350	20	701.11622	2	2143.67288	4
6 5 1	476.95525	12	1674.44924	16	701.11700	2	2143.67381	4
6 6 1	570.29268	16	1778.41999	22	862.22648	4	2321.85520	10
6 6 0	570.29271	14	1778.41995	18	862.22687	4	2321.85509	6

(continued on next page)

the figure. The resulting experimental line lists with assignments, which include 1155 and 1306 transitions for D₂¹⁸O and HD¹⁸O, respectively, are attached to this paper as **Supplementary materials**. A number of strong and middle-intensity experimental lines of interest are blended by absorption of other water isotopologues or saturated in our spectra, and then dropped from the list. On this reason, full transition lists have been generated in the considered spectral region for HD¹⁸O and D₂¹⁸O molecules using precise upper and lower energy levels derived in this study (see the following section), and PS line intensities. These lists are also provided as **Supplementary material** to this paper.

As we are interested in the determination of the rotational levels of two lowest vibrational states only, we will not describe here in details the procedure of rotation-vibrational transitions validating and processing which is similar to that in [1,3], as this will be a subject of future studies planned by the International Union of Pure and Applied Chemistry (IUPAC) task group [2,3].

Table 2 (continued)

$J_{Ka Kc}$		$D_2^{18}O$				$HD^{18}O$				
		(0 0 0)		(0 1 0)		(0 0 0)		(0 1 0)		
		E^{OBS}	δE	E^{OBS}	δE	E^{OBS}	δE	E^{OBS}	δE	
7	0	7	303.34067	16	1473.20117	22	400.36333	2	1796.50592	2
7	1	7	303.56470	10	1473.52405	14	401.57381	2	1798.04440	2
7	1	6	362.02089	14	1535.80377	22	470.93811	2	1873.24272	2
7	2	6	366.55016	10	1541.79495	14	486.80393	2	1892.28373	2
7	2	5	399.57652	14	1575.44492	22	516.79903	2	1923.69038	4
7	3	5	423.40998	10	1604.27712	14	572.12817	2	1987.44896	2
7	3	4	433.08181	14	1613.33778	16	577.34773	2	1992.58832	2
7	4	4	486.14412	12	1674.43030	12	676.81767	2	2104.63729	2
7	4	3	487.14923	14	1675.28203	16	677.11895	2	2104.91763	2
7	5	3	563.33936	14	1760.91805	14	809.31715	2	2252.22137	2
7	5	2	563.38173	16	1760.95117	20	809.32462	2	2252.22810	4
7	6	2	656.56881	14	1864.82410	18	969.90070	4	2429.86196	6
7	6	1	656.56943	16	1864.82462	20	969.90086	4	2429.86185	4
7	7	1	764.88018	18	1984.84136	24	1157.47032	6	2635.92278	8
7	7	0	764.88041	22	1984.84148	26	1157.47036	6	2635.92297	8
8	0	8	385.25063	12	1554.70542	16	508.92972	2	1904.57377	4
8	1	8	385.34994	16	1554.85483	22	509.57563	2	1905.41554	2
8	1	7	455.01449	10	1629.44843	14	594.70702	2	1997.98408	4
8	2	7	457.49049	16	1632.88385	18	605.55010	2	2011.30532	2
8	2	6	502.90253	10	1679.59030	14	649.04983	2	2057.06023	4
8	3	6	520.46205	14	1701.57634	18	696.12360	2	2111.93807	2
8	3	5	537.99594	10	1718.30876	14	706.59869	2	2122.31989	2
8	4	5	585.16497	14	1773.55748	18	801.35920	2	2229.60850	2
8	4	4	587.91510	10	1775.91191	14	802.23305	2	2230.42239	2
8	5	4	662.25506	14	1859.91303	20	933.12340	4	2376.42114	4
8	5	3	662.42876	12	1860.04937	14	933.15523	2	2376.44936	4
8	6	3	755.25847	22	1963.64020	20	1093.02722	4	2553.36291	6
8	6	2	755.26372	18	1963.64403	18	1093.02767	4	2553.36306	6
8	7	2	863.56652	22	2083.70923	28	1279.99739	6	2758.80347	8
8	7	1	863.56641	16	2083.70892	18	1279.99774	6	2758.80308	6
8	8	1	985.95998	24	2218.59954	28	1492.93468	8	2991.19240	8
8	8	0	985.95967	20	2218.59938	22	1492.93506	8	2991.19235	12
9	0	9	476.68013	18	1645.61384	20	629.96928	4	2024.93989	4
9	1	9	476.72323	12	1645.68182	20	630.30543	4	2025.38904	4
9	1	8	557.09832	16	1732.05282	22	730.87595	2	2135.08257	4
9	2	8	558.37482	12	1733.90903	20	737.82016	2	2143.83909	4
9	2	7	616.68195	16	1794.46897	20	796.74981	2	2206.09838	2
9	3	7	628.58818	10	1810.03734	14	835.04799	2	2251.43223	2
9	3	6	656.47940	16	1837.12429	22	853.54655	2	2269.91732	2
9	4	6	696.41162	12	1884.97216	16	941.59441	2	2370.33950	4
9	4	5	702.68700	16	1890.43075	18	943.75952	2	2372.36006	2
9	5	5	773.71361	12	1971.44932	14	1072.57972	4	2516.31514	4
9	5	4	774.27947	14	1971.89676	18	1072.68836	4	2516.41164	4
9	6	4	866.39041	12	2074.89120	18	1231.63192	10	2692.38010	6
9	6	3	866.41624	16	2074.91017	12	1231.63317	6	2692.38186	6
9	7	3	974.60025	16	2194.92412	18	1417.86661	10	2897.06346	8
9	7	2	974.60067	20	2194.92448	18	1417.86782	6	2897.06398	8
9	8	2	1097.10683	18	2329.98982	32	1630.10338	10	3128.72162	14
9	8	1	1097.10720	10	2329.98998	32	1630.10461	8	3128.72146	12
9	9	1	1232.65596	28	2478.56992	26	1867.33591	46	3385.98912	24
9	9	0	1232.65609	32	2478.57017	26	1867.33583	28	3385.98927	24
10	0	10	577.63573	14	1745.93966	18	763.51363	4	2157.64484	6
10	1	10	577.65471	20	1745.97057	24	763.68509	4	2157.88040	4
10	1	9	668.37532	14	1843.69028	18	879.09933	4	2284.10678	4
10	2	9	669.00849	18	1844.65442	22	883.31073	4	2289.56494	4
10	2	8	739.93212	14	1919.02133	16	958.94111	4	2369.83402	4
10	3	8	747.36502	18	1929.23220	22	988.54292	4	2405.56980	4
10	3	7	787.59463	14	1968.92706	16	1017.97492	4	2435.24000	4
10	4	7	819.57541	18	2008.39557	22	1097.41708	4	2526.73224	4
10	4	6	831.84164	14	2019.29610	20	1102.13870	4	2531.15682	4
10	5	6	897.67756	18	2095.50311	22	1227.71925	6	2671.93518	4
10	5	5	899.22489	12	2096.73631	16	1228.03537	6	2672.21536	4
10	6	5	989.98990	20	2198.59540	20	1385.73591	18	2846.93445	8
10	6	4	990.08634	14	2198.66648	18	1385.74699	16	2846.94455	8
10	7	4	1097.98387	10	2318.48250	28	1571.08747	22	3050.70815	14
10	7	3	1097.98700	18	2318.48338	14	1571.08734	20	3050.70795	12
10	8	3	1220.53557	24	2453.66225	28	1782.50339	22	3281.51309	16
10	8	2	1220.53571	22	2453.66231	18	1782.50330	20	3281.51334	16
10	9	2	1356.31591	34	2602.54239	38	2018.90714	38	3537.90803	34
10	9	1	1356.31593	26	2602.54243	36	2018.90746	34	3537.90761	34
10	10	1	1504.07350	44	2763.64111	44	2279.40956*	52	3818.73049	38
10	10	0	1504.07343	44	2763.64098	42	2279.40927*	50	3818.73057	64

Table 2 (continued)

$J_{Ka Kc}$			$D_2^{18}O$				$HD^{18}O$			
			(0 0 0)		(0 1 0)		(0 0 0)		(0 1 0)	
			E^{OBS}	δE	E^{OBS}	δE	E^{OBS}	δE	E^{OBS}	δE
11	0	11	688.11286	24	1855.68268	26	909.56903	8	2302.70453	10
11	1	11	688.12059	16	1855.69663	22	909.65513	8	2302.82631	8
11	1	10	788.95752	22	1964.48380	22	1039.31865	8	2444.94619	6
11	2	10	789.26419	14	1964.97152	20	1041.76688	8	2448.20897	6
11	2	9	872.08524	24	2052.51293	22	1134.59365	6	2547.20686	6
11	3	9	876.40911	14	2058.76332	22	1156.21549	6	2573.94963	6
11	3	8	930.22506	22	2112.65155	22	1199.28328	8	2617.73636	6
11	4	8	954.26270	16	2143.45867	20	1268.63563	8	2698.60444	6
11	4	7	975.27916	24	2162.59303	30	1277.85519	18	2707.30175	4
11	5	7	1034.02554	16	2231.97698	14	1398.55039	28	2843.29068	6
11	5	6	1037.68623	20	2234.93148	22	1399.35823	28	2844.00682	6
11	6	6	1126.06687	18	2334.76013	14	1555.36641	18	3017.04556	16
11	6	5	1126.36856	24	2334.98363	18	1555.40405	18	3017.07714	14
11	7	5	1233.71882	18	2454.37312	20	1739.66130	26	3219.73492	18
11	7	4	1233.73341	26	2454.38301	24	1739.66214	24	3219.73621	24
11	8	4	1356.22389	26	2589.58633	34	1950.12627	28	3449.55549*	26
11	8	3	1356.22401	32	2589.58622	32	1950.12643	30	3449.55568	26
11	9	3	1492.18801	34	2738.72623	36	2185.59031	42	3704.96589	34
11	9	2	1492.18786	48	2738.72625	40	2185.59034	40	3704.96581	36
11	10	2	1640.29705	40	2900.25271	42	2445.11174*	60	3984.74712	52
11	10	1	1640.29696	44	2900.25260	52	2445.11212*	62	3984.74679	52
11	11	1	1799.31429	72	3072.72811	60			4287.91433	62
11	11	0	1799.31414	80	3072.72818	60			4287.91462	64
12	0	12	808.09882	22	1974.83352	28	1068.12425	10	2460.11496	8
12	1	12	808.10205	28	1974.84017	32	1068.16700	10	2460.17755	8
12	1	11	918.91462	18	2094.52313	20	1211.60753	8	2617.66274	8
12	2	11	919.06084	26	2094.76632	34	1212.98590	8	2619.55322	8
12	2	10	1013.02147	16	2194.66720	22	1322.76128	10	2737.20148	10
12	3	10	1015.40776	24	2198.29132	26	1337.66582	22	2756.16005	10
12	3	9	1083.18882	20	2267.12827	22	1396.62024	16	2816.57123	12
12	4	9	1100.03517	26	2289.73759	24	1454.97301	18	2885.68709	10
12	4	8	1132.35987	22	2319.87483	18	1471.27148	14	2901.20727	10
12	5	8	1182.53686	26	2380.68434	26	1585.03903	30	3030.35156	14
12	5	7	1190.14910	20	2386.94188	18	1586.89562	30	3031.99930	12
12	6	7	1274.59976	30	2483.36798	26	1740.54185	22	3202.72652	14
12	6	6	1275.41983	20	2483.97914	18	1740.65001	22	3202.81797	18
12	7	6	1381.80316	30	2602.59049	28	1923.59251	28	3404.14311*	38
12	7	5	1381.85429	20	2602.62557	22	1923.59507	42	3404.14473	24
12	8	5	1504.14871	36	2737.73070	42	2132.96094*	52	3632.83348	44
12	8	4	1504.15017	28	2737.73192	26	2132.96171	44	3632.83284	50
12	9	4	1640.22982	54	2887.07208	48	2367.36819	46	3887.13963	38
12	9	3	1640.23013	32	2887.07232	32	2367.36788	44	3887.13996	38
12	10	3	1788.65883	46	3048.99942	54			4165.77100	56
12	10	2	1788.65913	36	3048.99964	38			4165.77097	58
12	11	2	1948.15242	62	3222.03326	92			4467.72468	78
12	11	1	1948.15263	50	3222.03335	82			4467.72430	72
12	12	1	2117.48828	144	3404.78836	92				
12	12	0	2117.48837	128	3404.78851	86				
13	0	13	937.57799	34	2103.37895	36	1239.15655	10	2629.85808	12
13	1	13	937.57904	28	2103.38159	28	1239.17820	10	2629.88980	12
13	1	12	1058.27746	30	2233.85734	30	1396.05625	26	2802.35954	10
13	2	12	1058.34652	24	2233.97751	30	1396.81437	18	2803.42988	10
13	2	11	1162.85571	32	2345.52997	28	1522.77767	22	2939.03737	22
13	3	11	1164.12638	24	2347.55282	24	1532.51319	18	2951.80289	14
13	3	10	1245.44797	30	2431.23492	32	1608.98013	18	3030.73913	16
13	4	10	1256.45309	22	2446.79224	22	1656.07837	22	3087.63534	16
13	4	9	1302.08705	32	2490.27066	30	1682.42021	26	3113.00435	18
13	5	9	1342.89397	24	2541.34376	24	1787.09197	24	3233.03022	18
13	5	8	1356.94713	34	2553.18311	32	1790.98128*	26	3236.49388	22
13	6	8	1435.51526	24	2644.36096	22	1941.26896	46	3403.97996	24
13	6	7	1437.49270	36	2645.84756	32	1941.55193	40	3404.21778	28
13	7	7	1542.22865	26	2763.11727	26	2122.87937	54	3603.92287	32
13	7	6	1542.38310	40	2763.22474	34	2122.89139	68	3603.93318	46
13	8	6	1664.28408	28	2898.05967	26	2330.99381	62	3831.32471	34
13	8	5	1664.29193	44	2898.06453	42	2330.99245	70		
13	9	5	1800.39733	40	3047.52594	32	2564.21863	86	4084.40377	60
13	9	4	1800.39754	62	3047.52451	48	2564.21927	70	4084.40300	72
13	10	4	1949.09809	42	3209.81369	52			4361.77464	56
13	10	3	1949.09806	64	3209.81340	66			4361.77495	62
13	11	3	2109.04718	64	3383.38998	46				
13	11	2	2109.04691	74	3383.38968	56				
14	0	14	1076.53162	34	2241.30160	36	1422.63531	14	2811.90786	12

(continued on next page)

Table 2 (continued)

$J_{Ka Kc}$			$D_2^{18}O$				$HD^{18}O$			
			(0 0 0)		(0 1 0)		(0 0 0)		(0 1 0)	
			E^{OBS}	δE	E^{OBS}	δE	E^{OBS}	δE	E^{OBS}	δE
14	1	14	1076.53210	50	2241.30236	56	1422.64530	14	2811.92369	14
14	1	13	1207.05217	30	2382.50616	28	1592.72667	24	2999.11876	18
14	2	13	1207.08451	40	2382.56525	38	1593.13622	24	2999.71494	26
14	2	12	1321.74102	28	2505.25433	26	1734.34015	22	3152.29578	16
14	3	12	1322.40183	36	2506.35525	34	1740.41596	28	3160.51641	18
14	3	11	1416.35617	30	2604.12626	26	1835.26122	28	3259.13108	22
14	4	11	1423.11360	36	2614.20416	32	1871.54861	40	3304.04640	26
14	4	10	1483.28859	30	2672.67931	28	1910.90460	28	3342.40519	24
14	5	10	1514.70180	36	2713.59220	36	2004.53940*	36	3451.17010	24
14	5	9	1537.98919	28	2733.77587	26	2012.02936	32	3457.87799	30
14	6	9	1608.66687	38	2817.61851	32	2157.53605	42	3620.78953	36
14	6	8	1612.95131	28	2820.88362	28	2158.20800	38	3621.35652	30
14	7	8	1714.96947	40	2935.92519	44	2337.51942	56	3819.06526	38
14	7	7	1715.38538	30	2936.21616	30	2337.55592	94	3819.09292	64
14	8	7	1836.60314	46	3070.53766	44	2544.20305	232	4045.00325	82
14	8	6	1836.62927	36	3070.55387	32	2544.20441	230	4045.00453	74
14	9	6	1972.64335	60	3220.03065	54			4296.72021	82
14	9	5	1972.64410	40	3220.03120	36			4296.72157	72
14	10	5	2121.55136	80	3382.62294	70				
14	10	4	2121.55170	48	3382.62273	48				
14	11	4	2281.92008	82						
14	11	3	2281.92059	72						
15	0	15	1224.93847	52	2388.58353	54	1618.52279	50	3006.23097	16
15	1	15	1224.93881	42	2388.58307	40	1618.52806	44	3006.23887	16
15	1	14	1365.23156	46	2540.46950	44	1801.64481	30	3207.98589	28
15	2	14	1365.24671	38	2540.49919	36	1801.86293	26	3208.31383	28
15	2	13	1489.78576	46	2673.97921	42	1957.42643	34	3376.88151	24
15	3	13	1490.12464	34	2674.56915	34	1961.08412	32	3381.98912	24
15	3	12	1595.72339	42	2785.39591	44	2074.36200	40	3500.60435	30
15	4	12	1599.67827	32	2791.60669	32	2100.95388	38	3534.47927	32
15	4	11	1674.74858	50	2865.90440	40	2155.95554	32	3588.72452	48
15	5	11	1697.52477	32	2897.01420	30	2237.13408	48	3684.53473	28
15	5	10	1732.66344	46	2928.36089	44	2250.44841	86	3696.56337	60
15	6	10	1793.82393	38	3002.94720	34	2389.29886	218	3853.11112	44
15	6	9	1802.21712	54	3009.47040	44			3854.35476	46
15	7	9	1899.97164	36	3120.96452	40	2567.50167	174	4049.54646	46
15	7	8	1900.98182	50	3121.67593	66			4049.62231	60
15	8	8	2021.07348	44	3255.12071	36			4273.83998	110
15	8	7	2021.14946	88	3255.17279	72			4273.84218	72
15	9	7	2156.91595	50	3404.52749	44			4524.05407	242
15	9	6	2156.91722	116	3404.52964	54			4524.05271	244
15	10	6	2305.95363	70	3567.35171	56				
15	10	5			3567.35096	72				
15	11	5	2466.69489	142						
15	11	4	2466.69438	154						
16	0	16	1382.77755	50	2545.20125	48	1826.77946	56	3212.79009	46
16	1	16	1382.77830	66	2545.20127	56	1826.77961	64	3212.79345	50
16	1	15	1532.79866	46	2707.74017	44	2022.80780	42	3428.97648	44
16	2	15	1532.80602	56	2707.75472	54	2022.92264	38	3429.15480	38
16	2	14	1667.05104	44	2851.79260	42	2192.14279	100	3612.87858	36
16	3	14	1667.22291	54	2852.10578	52	2194.28438	42	3615.96567	44
16	3	13	1783.64693	42	2975.01293	40	2325.33304	54	3754.11909	32
16	4	13	1785.88401	52	2978.70187	50	2343.86226	60	3778.51212	40
16	4	12	1875.38204	50	3068.78123	48	2416.57199	136	3850.99751	54
16	5	12	1890.92161	66	3091.17192	60	2484.54560	218	3932.80790	38
16	5	11	1939.98230	56	3136.13557	42	2506.47077	74	3952.85244	48
16	6	11	1990.67035	72	3200.07301	70	2636.46447	118	4100.85547	102
16	6	10	2005.60040	54	3211.98185	48			4103.39944	62
16	7	10	2097.13558	58	3318.15220	66				
16	7	9	2099.37737	56	3319.74311	48			4295.52502	234
16	8	9	2217.65717	84	3451.76471	58				
16	8	8	2217.86078	130					4517.80283	186
16	9	7	2353.17657	82	3600.96179	52				
17	0	17	1550.02369	80	2711.13628	78	2047.35625	62	3431.54527	70
17	1	17	1550.02376	62	2711.13581	56	2047.35741	52	3431.54655	76
17	1	16	1709.73361	70	2884.30108	62	2256.19483	74	3662.08041	44
17	2	16	1709.73722	56	2884.30787	56	2256.25448	66	3662.17734	50
17	2	15	1853.55863	64	3038.74061	64	2438.60560	46	3860.45854	48
17	3	15	1853.64589	58	3038.90637	50	2439.83330	52	3862.24590	314
17	3	14	1980.30020	70	3173.12590	60	2587.54188	188	4018.89370	48
17	4	14	1981.53745	50	3175.26314	56	2599.87018	304		
17	4	13	2084.45040	76	3280.36401	66			4128.11844	48

Table 2 (continued)

$J_{Ka Kc}$			$D_2^{18}O$				$HD^{18}O$			
			(0 0 0)		(0 1 0)		(0 0 0)		(0 1 0)	
			E^{OBS}	δE	E^{OBS}	δE	E^{OBS}	δE	E^{OBS}	δE
17	5	13	2094.48368	82	3295.64628	72		4195.60305	126	
17	5	12	2158.76776	72	3356.02320	104		4226.75672	68	
17	6	12	2198.82502	60	3408.63630	88		4363.87623	86	
17	6	11	2223.05595	88	3428.58329	82		4368.74926	232	
17	7	11	2306.30122	78	3527.35087	66				
17	7	10	2310.86959	88				4556.81893	132	
17	8	10			3660.41277	66				
18	0	18	1726.65382	72	2886.36203	70	2280.21107	150	3662.44807	72
18	1	18	1726.65439	92	2886.36196	88	2280.21107	150	3662.44749	76
18	1	17	1896.01183	70	3070.13347	66	2501.76756	58	3907.27633	76
18	2	17	1896.01182	164	3070.13673	76	2501.79845	64	3907.32908	88
18	2	16	2049.30928	68	3234.84046	68	2696.89619	148		
18	3	16	2049.35317	78	3234.92798	80	2697.58978	118		
18	3	15	2185.82989	68	3379.90509	58				
18	4	15	2186.50473	98	3381.12268	80				
18	4	14	2301.65934	142	3500.09205	154				
18	5	14			3510.05152	108				
18	5	13	2387.79678	146	3586.84207	208				
18	6	13	2417.86459	126						
18	6	12	2454.06272	196						
18	7	12	2527.23526	112						
19	0	19	1912.63700	120	3070.85720	116	2525.29056	84	3905.45821	158
19	1	19	1912.63708	98	3070.85663	98	2525.29027	76	3905.45821	158
19	1	18			3265.21641	170				
19	2	18	2091.60750	84	3265.21642	78				
19	2	17			3440.08686	98				
19	3	17	2254.31152	128	3440.13328	76				
19	3	16	2400.32450	160						
19	4	16	2400.69126	108	3596.16662	86				
19	4	15	2527.04556	112						
19	5	15	2530.74889	144						
19	5	14	2625.95201	96						
19	6	14	2647.35485	136						
20	0	20	2107.94994	120						
20	1	20	2107.95051	134						
20	1	19	2296.48967	114	3469.52329	94				
20	2	19	2296.48963	160						
21	0	21	2312.55961	172	3467.53855	142				
21	1	21	2312.55967	148	3467.53798	128				
21	2	20	2510.63256	152						
21	4	18	2856.46917	174						
22	0	22	2526.43680	176	3679.67075	158				
22	1	22	2526.43737	186	3679.67069	184				
22	1	21			3905.70926	162				

Note: $J_{Ka Kc}$ – rotational quantum numbers; E^{OBS} – experimental energies, cm^{-1} ;
 δE – experimental energy uncertainties, 10^{-5}cm^{-1} ;
Energy levels marked by asterisk differ importantly from Ref. [1] data.

3.2. Energy levels determination and modeling for $D_2^{18}O$ molecule

Initial set of processed transitions consisted of 5502 entries coming from 10 original sources [4,5,11–17] shown in Table 1. These transitions have been checked against PS calculations, and then the consistency of the combination differences has been examined. As a result, 53 transitions (21 from Ref. [17] and 32 from Ref. [15], see also comments included in [4,5]) have been excluded from consideration as being in difference from 0.03 to 1.43cm^{-1} with those calculated from obtained experimental energy levels, and they are believed to be incorrect. At the second step of analysis, 194 more transitions (see Table 1) have been removed from the energy levels determination on the reason of poor experimental accuracy revealed from the inspecting the combination differences relations. For a given combination difference (CD), energy level derived from the rejected transition deviated from the averaged value far from declared experimental uncertainty.

As a result of processing the weighted experimental frequencies, 302 energy levels for the ground state and 290 energy levels for the (0 1 0) state have been derived, which are included in

Table 2 together with their experimental uncertainties. Despite the fact that the $D_2^{18}O$ rotation-vibrational transitions have been studied at least in nine papers (see Table 1), the experimental energy levels for the (0 0 0) and (0 1 0) states have been presented only in [5,14]. The energy levels derived here for the ground state are in a very good agreement with our earlier data [5], where 286 energy levels have been reported. RMS deviation between the two (0 0 0) sets is 0.0006cm^{-1} . Concerning the (0 1 0) set, we could improve and enlarge the previous (0 1 0) set [14], where only 136 energy levels have been derived.

The newly obtained (0 0 0) and (0 1 0) energy levels have been introduced into the least squares fitting using rotational Hamiltonian written through the generating function G [18]:

$$H_{rot}^G = \sum_{n,m} g_{nm} J^{2n} \{G(\alpha^{(J)})\}^m + \sum_{n,m} u_{nm} J^{2n} [(J_+^2 + J_-^2), \{G(\alpha^{(J)})\}^m]_+, \quad (1)$$

where the generating function is defined according to [19] $G(\alpha^{(J)}) = (2/\alpha^{(J)})\{\sqrt{1 + \alpha^{(J)}J_z^2} - 1\}$. The J -dependence of $\alpha^{(J)}$ in the generating function is given by the development $\alpha^{(J)} = \sum_n \alpha_n J^{2n}$.

Table 3
Fitted values of the parameters of effective Hamiltonian for the ground and (0 1 0) states of HD¹⁸O and D₂¹⁸O.

Parameter	HD ¹⁸ O		D ₂ ¹⁸ O	
	(0 0 0) Value	(0 1 0) Value	(0 0 0) Value	(0 1 0) Value
$g_{00} \times E_{VV}$		1396.26654(15)		1170.15747(11)
$\alpha_0 \times 10^2$	0.661(15)	1.1427 ₇ (21)	1.249 ₄ (18)	27.64 ₉ (31)
$\alpha_1 \times 10^5$	0.892 ₈ (12)	-1.06 ₂ (11)	1.511 ₂ (14)	32.40 ₆ (37)
$\alpha_3 \times 10^{11}$				2.322 ₉ (68)
g_{10}	7.7100366 ₉ (35)	7.7354763(71)	6.0416151 ₆ (22)	6.0461029 ₆ (52)
$g_{20} \times 10^4$	-3.53685 ₆ (72)	-4.05384 ₁ (87)	-3.08816 ₂ (26)	-33.4478 ₁ (78)
$g_{30} \times 10^8$	4.054 ₈ (49)	6.395(35)	6.277 ₁ (13)	75.06 ₅ (45)
$g_{40} \times 10^{11}$	-0.92 ₁ (10)		-1.478 ₅ (21)	-18.19 ₄ (85)
$g_{50} \times 10^{14}$		-3.61 ₀ (16)		
g_{01}	15.400219(26)	17.430962 ₃ (64)	9.031906 ₈ (17)	10.209880 ₉ (36)
$g_{11} \times 10^3$	-1.27859 ₉ (77)	-1.1131 ₅ (18)	1.49098 ₂ (36)	18.5893 ₃ (92)
$g_{21} \times 10^6$	2.5012(71)	4.791 ₆ (17)	-0.2419(22)	0.548 ₁ (67)
$g_{31} \times 10^9$	-1.365 ₅ (21)	-2.093 ₈ (55)	0.1328 ₃ (39)	3.62 ₇ (16)
$g_{02} \times 10^2$	1.358 ₄ (56)	2.7394 ₉ (87)	1.935 ₆ (41)	57.19 ₅ (79)
$g_{12} \times 10^5$	2.366 ₅ (49)	-6.71 ₄ (48)	3.643 ₂ (36)	90.2 ₈ (10)
$g_{22} \times 10^8$	-2.362(23)	-8.867 ₉ (58)		
$g_{32} \times 10^{11}$		3.09 ₆ (12)		
$g_{03} \times 10^5$	0.611 ₁ (77)		-3.803 ₉ (80)	-146.1 ₂ (21)
$g_{13} \times 10^7$		3.65 ₄ (11)	-0.6172 (86)	-24.57 ₁ (33)
$g_{23} \times 10^{11}$	8.37 ₉ (14)	94.6(14)		
$g_{04} \times 10^8$	-2.44 ₅ (18)	-15.54 ₇ (40)	1.506 ₇ (40)	29.1 ₁ (29)
$g_{14} \times 10^9$		-2.892 ₇ (76)		
$g_{24} \times 10^{12}$		-1.898 ₃ (89)		
$g_{05} \times 10^{10}$		16.37 ₃ (79)	0.309 ₃ (24)	65.9 ₁ (25)
$g_{15} \times 10^{12}$		3.29 ₃ (16)		
$u_{00} \times 10^1$	6.745856 ₉ (33)	7.287240 ₅ (44)	6.157813 ₆ (15)	6.4547954 ₂ (32)
$u_{10} \times 10^4$	-1.18546 ₃ (53)	-1.44741 ₃ (51)	-1.23147 ₈ (17)	-1.36191 ₆ (48)
$u_{20} \times 10^8$	2.126 ₁ (29)	3.190 ₃ (16)	3.1440 ₄ (75)	3.799 ₉ (25)
$u_{30} \times 10^{12}$	-5.095(53)		-7.64 ₆ (11)	-9.28 ₈ (44)
$u_{50} \times 10^{17}$		-2.95 ₃ (14)		
$u_{01} \times 10^3$	-2.09366(96)	-3.4986(18)	-0.32041 ₇ (20)	-0.70883(56)
$u_{11} \times 10^7$	10.821 ₂ (74)	15.40 ₂ (19)	-0.8500 ₄ (65)	-1.458 ₅ (45)
$u_{21} \times 10^{10}$	-8.22 ₂ (16)	-14.93 ₉ (28)		-1.48 ₉ (11)
$u_{02} \times 10^5$	1.3206 ₅ (86)	4.327 ₄ (11)	0.25841 ₅ (67)	0.4986 ₆ (27)
$u_{12} \times 10^9$	-1.59 ₉ (19)	12.33 ₉ (47)		
$u_{22} \times 10^{12}$			1.007 ₇ (45)	7.04 ₄ (14)
$u_{03} \times 10^8$	-9.10 ₁ (10)	-66.62 ₉ (83)		
$u_{13} \times 10^{11}$	-7.72 ₈ (23)			1.36 ₅ (20)
$u_{04} \times 10^{10}$		39.3 ₅ (15)	-0.650 ₂ (34)	1.294 ₆ (43)
$u_{24} \times 10^{16}$			1.570 ₃ (73)	
$u_{05} \times 10^{13}$			4.41 ₁ (18)	

Note: All linear parameters g_{nm} and u_{nm} are in cm^{-1} . Non-linear parameters α_n are dimensionless. 68% confidential intervals of parameters in last digits are given in parentheses.

Numerical parameters g_{nm} , u_{nm} , and α_n of Hamiltonian (1) are adjustable spectroscopic parameters. This representation of the rotational operator doesn't contain divergent series essential for the conventional perturbative approach, and proved to be much more accurate not only in the fitting, but also in the extrapolation calculations. Relations of the H_{rot}^G parameters with Watson's constants are discussed in [20]. Spectroscopic parameters of Hamiltonian (1) were determined in a least square fit to experimental rotational energies of each vibrational state.

As our dataset of rotational energies of the ground state was very close to that of Ref. [5], we used the spectroscopic parameters from [5] as the initial approximation in the fitting process. This time we attempted to vary all the parameters given in [5]. Finally, 293 of 302 experimental energy levels of the (0 0 0) state were fitted with RMS deviation of $2.4 \times 10^{-4} \text{ cm}^{-1}$ by varying 27 parameters. It is worth noticing that all the nine experimental energy levels excluded from the fitting are derived either from single line not supported by CD relation, or from experimentally unresolved lines formed by transitions coming on or originated from nearly degenerate levels. We believe that for all these nine excluded energy levels the calculated values given in Supplementary material II are more accurate than the experimental ones.

The fitting of energy levels for the (0 1 0) state was similar to that for the ground state: 282 energy levels and 29 fitted param-

eters, RMS equals to $3.2 \times 10^{-4} \text{ cm}^{-1}$. No resonance perturbations from the nearby states have been detected for the (0 1 0). Again, all the eight excluded experimental energy levels seem to have distorted values. The largest *obs-calc* discrepancy of -0.0114 cm^{-1} correspond to $J_{Ka Kc} = 17_6 1_2$ level derived from one single line position. The spectroscopic parameters of the (0 0 0) and (0 1 0) states obtained are presented in Table 3 together with 68% confidential intervals. The full sets of calculated energies of both (0 0 0) and (0 1 0) states are given in Supplementary material II.

3.3. Energy levels determination and modeling for HD¹⁸O molecule

Determination of the HD¹⁸O energy levels from simultaneous processing all published and validated rovibrational transitions has been performed recently in [1,3], and we used the list of HD¹⁸O transitions which has been composed from the same original sources, as in [3], and enlarged by 1313 transitions of the ν_2 band assigned in this study. The final list consisted of 10,242 entries that corresponds to 7424 spectral lines. After the validation procedure, described above, 1489 transitions have been excluded from consideration, mostly, due to poor experimental accuracy. Totally, 8753 transitions have been processed, including 7506 previously published data, what is sufficiently smaller than

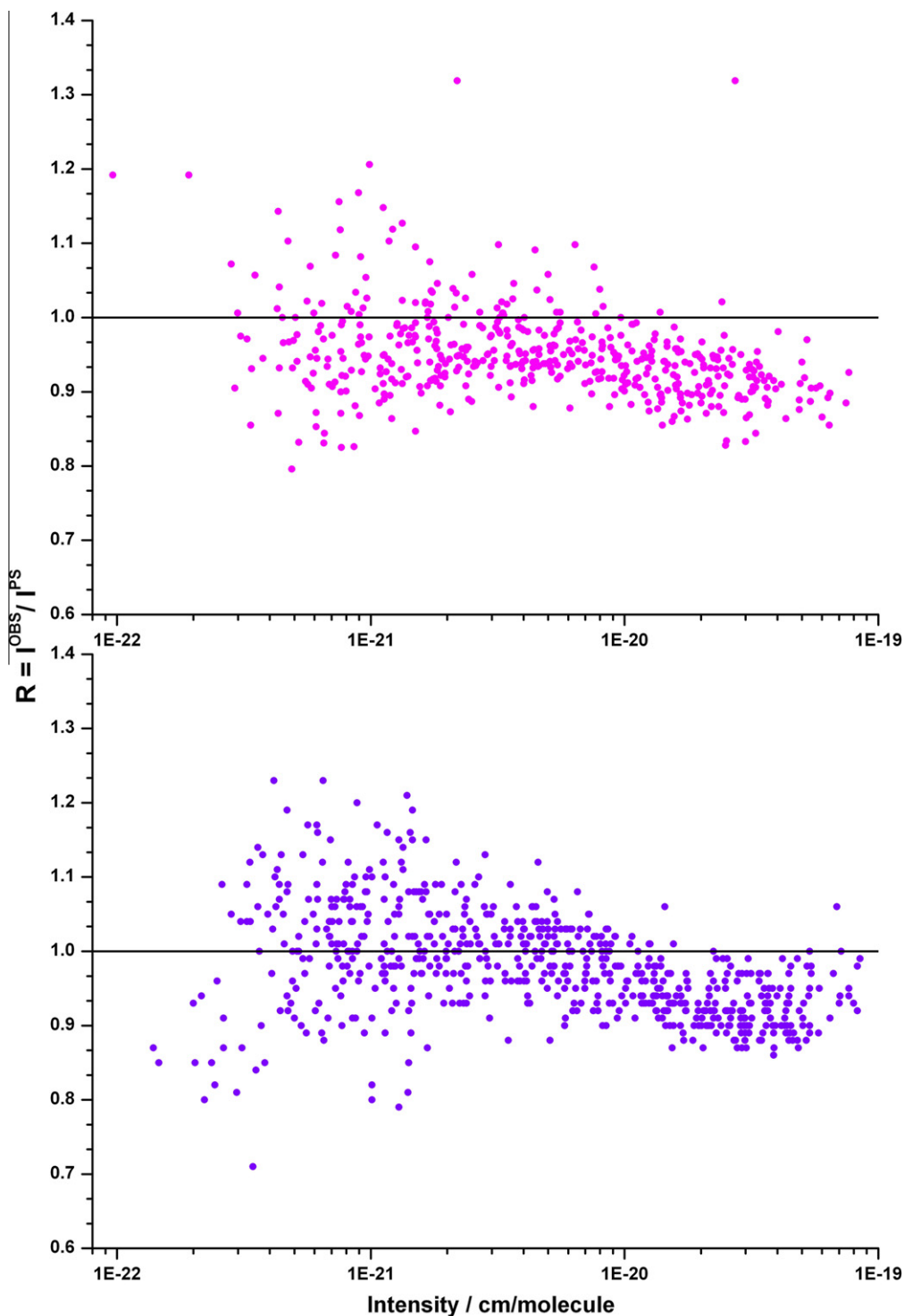


Fig. 3. Ratios of the observed (I^{OBS}) and calculated (I^{PS}) line intensities of D_2^{18}O (upper panel) and HD^{18}O (lower panel).

8729 transitions validated in [3]. This large difference in the number of validated transitions results from the fact that the computer code RITZ [1] exploited in this study doesn't make provision to enlarging the experimental uncertainties for the transitions-outliers, as MARVEL code does [21]. All the outliers (generally, deviating by more than 0.002 cm^{-1} from the values calculated by RITZ) are excluded manually. Finally 237 and 259 energy levels have been determined for the (0 0 0) and (0 1 0) states, respectively.

Modeling the HD^{18}O rotational energies of the ground vibrational state was close to that for D_2^{18}O : 227 experimental energy levels of 237 observed have been reproduced with $\text{RMS} = 2.6 \times 10^{-4}\text{ cm}^{-1}$ by varying 27 parameters. Again, most part of excluded experimental energy levels concerns nearly degenerate pairs. Most difficult case concerned modeling the rotational energies of the (0 1 0) state, since they are perturbed by resonance interactions with the (0 0 0), and (0 2 0) states. We did not account for these perturbations, and the fitting result is still acceptable:

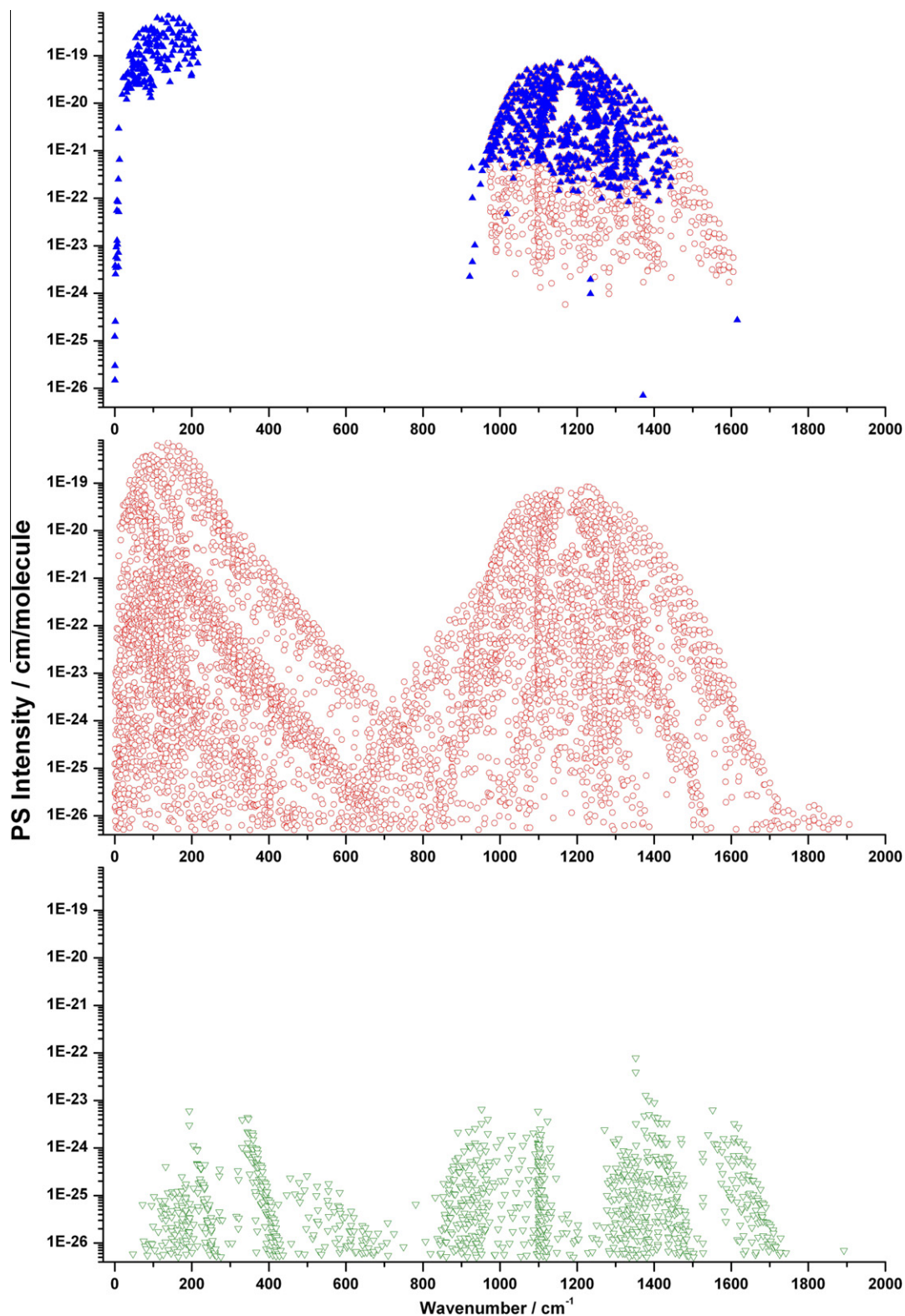


Fig. 4. Observed (upper panel), calculated from experimental energy levels (middle panel), and unobserved (lower panel) transitions of $D_2^{18}O$. Line positions on lower panel correspond to PS calculation [8].

246 energy levels of 259 observed have been modeled within RMS of $4.2 \times 10^{-4} \text{ cm}^{-1}$ by varying 33 parameters. Experimental energy levels of the (0 0 0) and (0 1 0) states of $HD^{18}O$ are shown in Table 2. The parameters obtained are included in Table 3. Full set of calculated rotational energies for the (0 0 0) and (0 1 0) states of $HD^{18}O$ are given in Supplementary material II.

Before present study, the most complete published sets of the (0 0 0) and (0 1 0) energy levels of $HD^{18}O$ are included in [1,3]: 171 levels for the (0 0 0) and 156 levels for the (0 1 0) states. The present work gives 237 levels for the ground state and 259 for the (0 1 0) state. Comparison of our data with those presented in [1] shows that both sets agree well on average, with RMS deviation

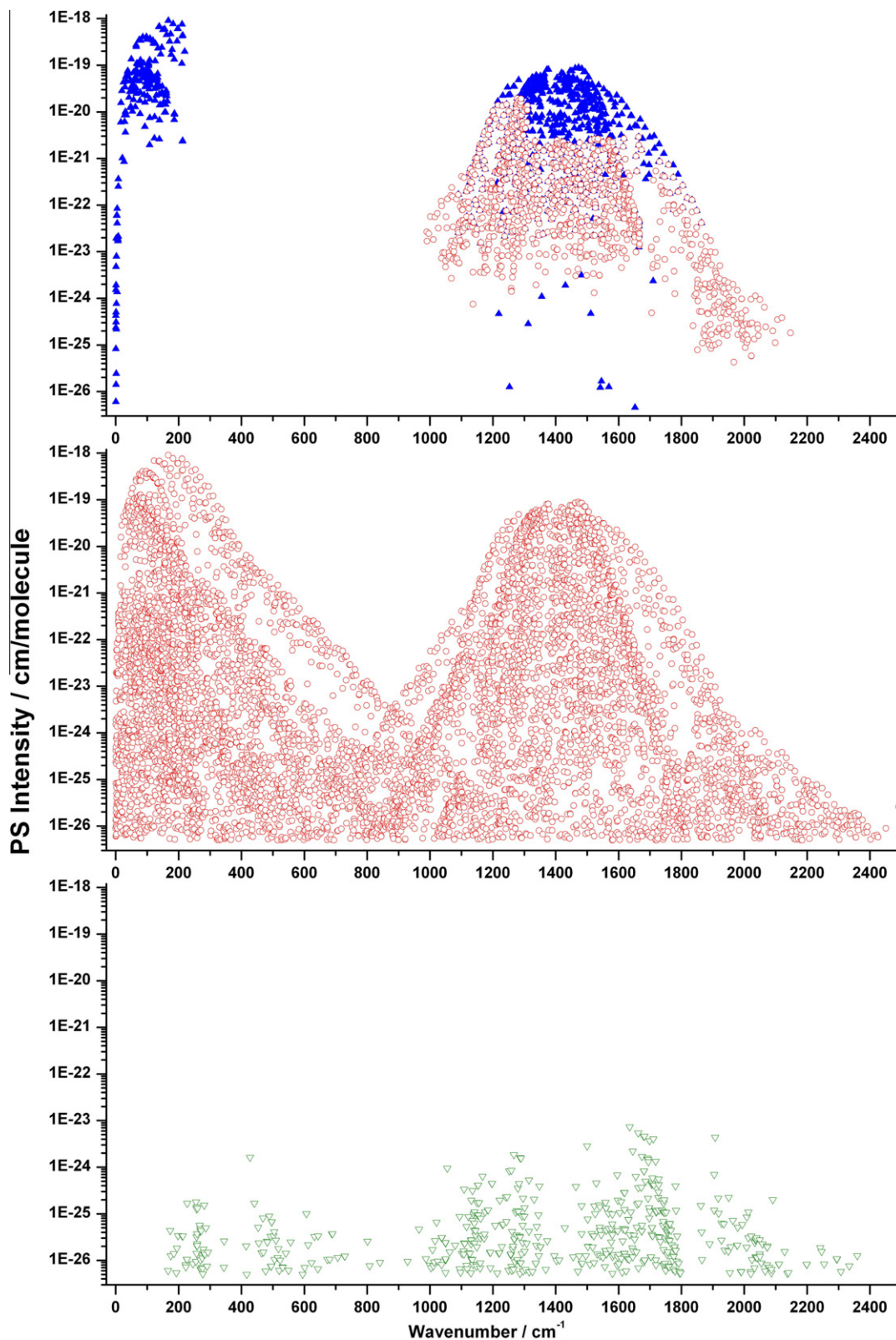


Fig. 5. Observed (upper panel), calculated from experimental energy levels (middle panel), and unobserved (lower panel) transitions of HD¹⁸O. Line positions on lower panel correspond to PS calculation [8].

of 0.0014 cm^{-1} for 318 levels. We did not confirm four energy levels from [1], they are marked by asterisk in Table 2. We also excluded five evident outliers from the comparison they also are marked by asterisk.

3.4. Trivial assignments

As it was already mentioned, part of strong and middle-intensity HD¹⁸O and D₂¹⁸O absorption lines of the ν_2 band have

been distorted due to overlapping with other transitions having comparable or larger intensities, and, consequently, have been deleted from the final lists. Complete absorption line list for the v_2 bands of considered molecules has been constructed by using the precise positions calculated from the experimental lower and upper levels derived in this study, and variational intensities [8]. As it was stated in [5], PS intensities for $D_2^{18}O$ agree very well with the experimental data [17] in the 2594–2918 cm^{-1} spectral region. Comparison of PS intensities of the v_2 band with the experimental values of Toth for $D_2^{18}O$ [14] and $HD^{18}O$ [22] is included in Fig. 3. Average ratio $R = I^{OBS}/I^{PS}$ equals to 0.98 for 734 line intensities of $HD^{18}O$ and to 0.95 for 515 line intensities of $D_2^{18}O$, confirming very high quality of PS intensities. However, the distribution of the intensity ratios is not symmetrical with respect to $R = 1$ value both for $D_2^{18}O$ and for $HD^{18}O$. It looks like the strongest experimental intensities being underestimated by about 5%.

Line lists of the transitions associated with experimental energy levels derived in this study with PS intensities over 5×10^{-27} cm/molecule include 5264 and 7429 entries for the $D_2^{18}O$ and $HD^{18}O$ molecules, respectively. The lists are attached to this paper as [Supplementary material III](#). Comparison of the previously observed transitions with those recorded in this paper and calculated from the experimental energy levels of the (0 0 0) and (0 1 0) states is shown in Figs. 4 and 5 for both studied molecules together with the residual unobserved lines. Closed triangles on the upper panels of Figs. 4 and 5 correspond to observed data from literature and open circles represent new measurements. Line list of the residual unobserved lines for both species is included in [Supplementary material IV](#).

4. Conclusion

Fourier transform absorption spectra of the $D_2^{18}O$ and $HD^{18}O$ molecules have been recorded and assigned based on variational and effective Hamiltonian calculations in the 970–2150 cm^{-1} spectral region. Precise energy levels (1088) of the (0 0 0) and (0 1 0) states including 302 new levels have been derived from 5255 rotation-vibrational transitions for the $D_2^{18}O$ and 8753 transitions for the $HD^{18}O$ molecules using fundamental Rydberg–Ritz principle. These energy levels have been modeled at a level of experimental accuracy with the effective Hamiltonian written through the generating functions. Detailed and precise lists of the line positions for the $D_2^{18}O$ and $HD^{18}O$ have been generated in the 0–2900 cm^{-1} spectral region, involving rotational and v_2 transitions. Line positions calculated from experimental energy levels were completed by variational (PS) line intensities. These lists can be used for various applications, in particular, for calibration purposes as well as for assignment of the high density hot spectra, investigations of the line profile, etc. List of variational lines not observed in 0–2900 cm^{-1} spectral region is composed from the PS database [8]

which can be useful in future experimental studies of the $HD^{18}O$ and $D_2^{18}O$ molecules.

Acknowledgments

This work was supported in part by RFBR (Russia, G. Nos. 09-05-93105, 10-05-93105 and 10-05-91176) and NNSF (China, G. Nos. 20903085 and 20873132), by the program 3.9 “Fundamental Optical Spectroscopy and Applications” of Russian Academy of Science, and by Chinese Ministry of Science and Technology (2007CB815203). S.N.M. acknowledges also support of Grant No. RUG1-2954-TO-09 of CRDF (USA) and Grant No. 09-05-92508-IK_a by RFBR. O.V.N. and S.N.M. gratefully acknowledge University of Science and Technology of China for visiting professorship and the support from Chinese Academy of Science. The authors also acknowledge Dr. S.A. Tashkun (Tomsk, Russia) for supplying his computer code RITZ which was used to determine experimental energy levels from observed line positions and for valuable discussions.

Appendix A. Supplementary data

Supplementary data associated with this article can be found, in the online version, at [doi:10.1016/j.jms.2010.10.007](https://doi.org/10.1016/j.jms.2010.10.007).

References

- [1] S.N. Mikhailenko, S.A. Tashkun, T.A. Putilova, E.N. Starikova, L. Daumont, A. Jenouvrier, et al., *J. Quant. Spectrosc. Radiat. Transfer* 110 (2009) 597–608.
- [2] J. Tennyson, P.F. Bernath, L.R. Brown, A. Campargue, M.R. Carleer, A.G. Császár, et al., *J. Quant. Spectrosc. Radiat. Transfer* 110 (2009) 573–596.
- [3] J. Tennyson, P.F. Bernath, L.R. Brown, A. Campargue, S. Fally, A.G. Császár, et al., *J. Quant. Spectrosc. Radiat. Transfer* 111 (2010) 2160–2184.
- [4] S.N. Mikhailenko, S.A. Tashkun, L. Daumont, A. Jenouvrier, M. Carleer, S. Fally, A.C. Vandaele, *J. Quant. Spectrosc. Radiat. Transfer* 111 (2010) 2185–2196.
- [5] H.-Y. Ni, A.-W. Liu, K.-F. Song, S.-M. Hu, O.V. Naumenko, T.V. Kruglova, S.A. Tashkun, *Mol. Phys.* 106 (2008) 1793–1801.
- [6] A.-W. Liu, J.-H. Du, K.-F. Song, L. Wang, L. Wan, S.-M. Hu, *J. Mol. Spectrosc.* 237 (2006) 149–162.
- [7] L.S. Rothman, I.E. Gordon, A. Barbe, D. Chris Benner, P.F. Bernath, M. Birk, et al., *J. Quant. Spectrosc. Radiat. Transfer* 110 (2009) 533–572.
- [8] <http://spectra.iao.ru>.
- [9] H. Partridge, D.W. Schwenke, *J. Chem. Phys.* 106 (1997) 4618–4639.
- [10] D.W. Schwenke, H. Partridge, *J. Chem. Phys.* 113 (2000) 6592–6597.
- [11] J. Bellet, W.J. Lafferty, G. Steenbeckeliens, *J. Mol. Spectrosc.* 47 (1973) 388–402.
- [12] J.W. Fleming, M.J. Gibson, *J. Mol. Spectrosc.* 62 (1976) 326–337.
- [13] J.W.C. Johns, *J. Opt. Soc. Am. B* 2 (1985) 1340–1354.
- [14] R.A. Toth, *J. Mol. Spectrosc.* 162 (1993) 41–54.
- [15] W.F. Wang, T.L. Tan, B.L. Tan, P.P. Ong, *J. Mol. Spectrosc.* 176 (1996) 226–228.
- [16] G. Di Lonardo, L. Fusina, *J. Mol. Spectrosc.* 135 (1989) 250–258.
- [17] R.A. Toth, *J. Mol. Struct.* 742 (2005) 49–68.
- [18] S.N. Mikhailenko, V.I. Tyuterev, G. Mellau, *J. Mol. Spectrosc.* 217 (2003) 195–211.
- [19] V.I. Tyuterev, *J. Mol. Spectrosc.* 151 (1992) 97–121.
- [20] V.I. Tyuterev, V.I. Starikov, S.A. Tashkun, S.N. Mikhailenko, *J. Mol. Spectrosc.* 170 (1995) 38–58.
- [21] T. Furtenbacher, A. Császár, J. Tennyson, *J. Mol. Spectrosc.* 245 (2007) 115–125.
- [22] R.A. Toth, *J. Mol. Spectrosc.* 162 (1993) 20–40.